6-1-2000

Gaussian Beams in Hollow Metal Waveguides

Lee W. Casperson
Portland State University

Citation Details

Lee W. Casperson, "Gaussian Beams in Hollow Metal Waveguides," J. Opt. Soc. Am. A 17, 1115-1123 (2000).

Gaussian beams in hollow metal waveguides

Lee W. Casperson

The Institute of Optics and The Rochester Theory Center for Optical Science and Engineering, University of Rochester, Rochester, New York 14627-0186

Received July 15, 1999; accepted February 15, 2000

Various families of Gaussian beams have been explored previously to represent the propagation of nearly plane electromagnetic waves in media having at most quadratic transverse variations of the index of refraction and the gain or loss in the vicinity of the beam. However, such beams cannot directly represent the wave solutions for propagation in planar or rectangular waveguides, and sinusoidal mode functions are more commonly used for such waveguides. On the other hand, it is also useful to consider the possibility of recurring Gaussian beams that have an approximately Gaussian transverse profile at certain distinct planes along the propagation path. It is shown here that under some conditions recurring Gaussian beams can describe wave propagation in hollow metal waveguides, and they can also lead to efficient coupling between the waveguide fields and free-space beams. © 2000 Optical Society of America [S0740-3232(00)00806-1]

OCIS codes: 230.0230, 230.7370, 230.7390, 350.5500.

1. INTRODUCTION

Gaussian beams have long been recognized as exact solutions of the paraxial wave equation for nearly plane waves propagating in media that have at most quadratic variations of the index of refraction and of the gain or loss in the vicinity of the beam. Thus at every reference plane along the beam propagation path the amplitude distribution remains Gaussian, while the phase fronts remain spherical. Because of this property, one might refer to these solutions as shape-invariant or *continuing* Gaussian beams. It was shown that Gaussian beams retain their basic functional form when propagating in free space,[1] real lenslike media,[2] complex lenslike media,[3] and other simple elements.[4] Off-axis polynomial-Gaussian beams have also been studied,[5] and their propagation in a range of complex and misaligned systems is now known.[6] Similar solution properties have been found to be shared by general families of Bessel–Gaussian, exponential-Gaussian, and trigonometric-Gaussian beams.[7]

Gaussian beams are especially useful for the long-distance propagation of optical-frequency fields in free space or in certain lenslike media. For lower-frequency fields the transverse dimensions of Gaussian beams may become too large, and more confining waveguiding systems are usually employed. Thus multiconductor transmission lines can be used for frequencies from dc up to the millimeter wave range (approximately $0-10^{11}$ Hz). For the higher microwave and millimeter-wave frequencies, hollow conducting cylinders of various cross-sectional shapes have proven to be useful (approximately $10^{10}-10^{13}$ Hz), and for field confinement at optical frequencies solid dielectric fibers are known to be very effective ($10^{14}-10^{15}$ Hz).

The best field confinement technology for the infrared region of the spectrum has been more difficult to determine ($10^{13}-10^{14}$ Hz). The fields of most widespread use in this range are those produced by the very efficient and powerful CO_2 lasers ($\lambda = 10.6\,\mu$m, $\nu = 2.83 \times 10^{13}$ Hz), which are employed in many areas of technology and medicine. To be specific, several citations to the CO_2 laser waveguide studies will be mentioned here, and similar but less extensive propagation studies have been conducted at other infrared wavelengths. Some success in the waveguiding of CO_2 wavelengths has been obtained by using solid media based on polycrystalline alkali halide fibers,[8–10] with transmission losses as low as 0.1 dB/m having been reported.[10] More commonly, the waveguides used to transmit CO_2 laser radiation are hollow, and of these some are uncoated dielectric tubes of plastic, glass, ceramic, or sapphire.[11–18] However, the greatest interest in hollow waveguides has centered on those in which the guiding surfaces are formed or deposited metal tubes. Materials for these tubes have included aluminum, copper, bronze, silver, or gold,[19–38] and again losses as low as 0.1 dB/m have been reported.[27,32]

None of the CO_2 waveguide types that have just been mentioned support continuing Gaussian beams. In particular, in waveguides with highly reflecting boundaries, near-Gaussian beams (some distortion must occur at boundaries) at one reference plane would not remain Gaussian at all other planes. As a result, it is usual to design such waveguides to operate with other electromagnetic field distributions. For example, it is common for rectangular waveguides to operate with sinusoidal mode functions, while the fields in circular waveguides may be expressed in terms of Bessel mode functions. These fields can match the corresponding waveguide boundary conditions and propagate with no change in their transverse distribution. In the case of waveguide amplifiers, these fields can also couple efficiently to the amplifying medium.

Sinusoidal or Bessel waveguide modes are, however, not without some disadvantages, especially for optical-frequency applications. In optical-frequency systems it is often necessary to couple free-space propagating beams into or out of waveguides. Most applications of waveguide laser amplifiers and oscillators require such beams, and thus transformations between waveguide and beam

0740-3232/2000/061115-09$15.00

field configurations are frequently needed. Such transformations never lead to the ideal field distributions that one might hope for, and they also may involve significant power loss. In this context, it is useful to consider the possibility of *recurring* Gaussian beams, which would have an approximately Gaussian transverse profile at more than one plane along the propagation path. It is shown here that under some conditions recurring (rather than continuing) Gaussian beams *can* describe wave propagation in hollow metal waveguides. Thus a metal waveguide of appropriate dimensions can efficiently transform a Gaussian input beam into a Gaussian output beam.

Paraxial propagation in a metal waveguide typically involves the grazing reflection of the guided fields from the interior waveguide surfaces. The grazing reflection of Gaussian beams from a single flat metal surface has recently been studied.[39] Those previous results are generalized here to include multiple reflections of Gaussian beams from the opposite pairs of plane waveguide surfaces in a plane-parallel or rectangular waveguide. It is shown numerically and analytically that a Gaussian beam at one reference plane in such a waveguide will recur at certain well-defined and easily calculated distances along the waveguide. These distances depend in part on the polarization of the fields with respect to the waveguide surfaces. If two of the points of Gaussian beam recurrence correspond to the ends of the waveguide, then the waveguide fields will have coupled efficiently to free-space Gaussian input and output beams.

A brief derivation of the Gaussian beam equations is included in Section 2. The purpose of this derivation is to reduce the partial differential wave equation to a set of first-order ordinary differential equations governing the various parameters that characterize the spatially evolving beam. The solutions of these simpler equations are discussed in Section 3 for off-axis Gaussian beam propagation in spatially homogeneous media. The application of these beams to recurring propagation in metal waveguides is explored in Section 4. For comparison and interpretation, the behavior of the more conventional sinusoidal waveguide modes is considered in Section 5.

2. BEAM EQUATIONS

One of the basic geometries to be considered here consists of a diffracting Gaussian beam injected between two parallel reflecting metal surfaces. The Gaussian beam is not necessarily injected at the center of the waveguide input plane, and it might also be propagating in part toward or away from one of the waveguide sides. This arrangement is shown in Fig. 1, and the coordinate system to be employed is also shown in the figure. Owing to diffraction and misalignment, the beam is assumed to interact with the waveguide surfaces over extended distances. The surfaces are assumed to be highly reflecting and flat, and with this restriction it is possible to obtain solutions that are not excessively cumbersome.

For any study of electromagnetic-wave propagation the fundamental starting point is the Maxwell–Heaviside equations. These equations can be combined to yield coupled equations that govern the various field components of a propagating electromagnetic beam. For the case of nearly plane waves in a medium in which the changes in permittivity and permeability per wavelength are small, the dominant transverse Cartesian field components are governed by the much simpler wave equation,

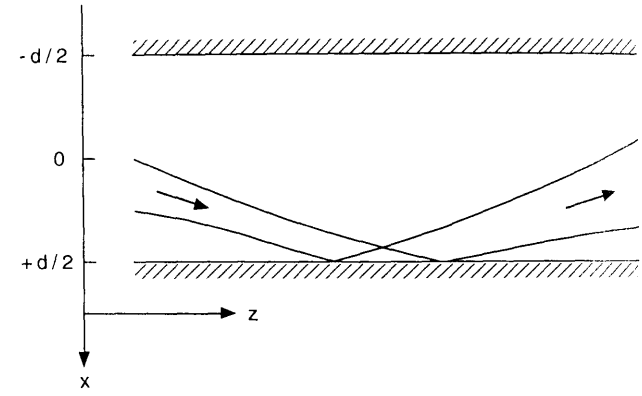

Fig. 1. Schematic representation of an off-axis Gaussian beam undergoing diffraction and reflection from the flat parallel surfaces of a waveguide. The coordinate system used in the analysis is also shown.

$$\nabla^2\mathbf{E}'(x, y, z) + k^2(x, y, z)\mathbf{E}'(x, y, z) = 0, \quad (1)$$

where $\mathbf{E}'$ is the complex amplitude of the electric field, and k is the potentially complex spatially dependent wave number. The wave number could, in principle, have an imaginary part due to nonzero conductivity or out-of-phase components of the polarization or magnetization. While Eq. (1) governs the dominant transverse components, the weak z components of the fields may be found at any time from the transverse components by means of the Maxwell–Heaviside equations.[40]

As noted above, a continuing Gaussian beam can propagate in spatially inhomogeneous media that have at most quadratic transverse variations in the vicinity of the beam. However, for applications of interest here it is assumed that the propagation medium within the waveguide is essentially a uniform dielectric, and thus k in Eq. (1) will be considered to be a constant within the waveguide. For consistency with Ref. 39, this constant will be represented as β_0. Furthermore, because of the separability of the wave equation for a uniform medium, no particular insight is gained by retaining propagation effects in both of the transverse directions. Thus we assume at the outset that there are no field variations in the y direction. For a linearly polarized wave that propagates primarily in the z direction, a useful substitution is

$$E'(x, y, z) = A(x, z)\exp(-i\beta_0 z), \quad (2)$$

where A is a new complex amplitude function. With this substitution Eq. (1) reduces to the paraxial wave equation

$$\frac{\partial^2 A}{\partial x^2} - 2i\beta_0\frac{\partial A}{\partial z} = 0, \quad (3)$$

where A is assumed to vary so slowly with z that its second derivative can be neglected.

A useful form for a fundamental astigmatic off-axis Gaussian beam is[40]

$$A(x, y, z) = A_0 \exp\left\{ -i\left[\frac{Q_x(z)x^2}{2} + S_x(z)x + P(z)\right]\right\}. \tag{4}$$

The size of the beam and the curvature of the phase fronts are governed by the complex beam parameter Q_x. The location of the beam depends on the complex displacement parameter S_x, and the phase and amplitude of the beam are governed by the complex phase parameter P. If Eq. (4) is substituted into Eq. (3), one finds by equating equal powers of x that the various parameters of the beam are governed by the following equations:

$$Q_x^2 + \beta_0 \frac{dQ_x}{dz} = 0, \tag{5}$$

$$Q_x S_x + \beta_0 \frac{dS_x}{dz} = 0, \tag{6}$$

$$\frac{dP}{dz} = -i\frac{Q_x}{2\beta_0} - \frac{S_x^2}{2\beta_0}. \tag{7}$$

The detailed significance of the parameter Q_x is contained in the relation

$$\frac{Q_x(z)}{\beta_0} = \frac{1}{q_x(z)} = \frac{1}{R_x(z)} - \frac{2i}{\beta_0 w_x^2(z)}, \tag{8}$$

where R_x and w_x are, respectively, the radius of curvature of the phase fronts and the $1/e$ amplitude spot size in the x direction. From Eq. (4), the ratio $d_{xa} = -S_{xi}/Q_{xi}$ is the displacement in the x direction of the amplitude center of the Gaussian part of the beam, and the ratio $d_{xp} = -S_{xr}/Q_{xr}$ is the displacement in the x direction of the phase center of the beam. Here the subscripts i and r denote, respectively, the imaginary and real parts of the parameters Q_x and S_x.

For our present purposes it is convenient to express the complex displacement parameter in terms of the more physically intuitive amplitude displacement and the rate of change of this displacement with the propagation distance z. Combining Eqs. (5) and (6) with the displacement definitions, one obtains the relation[41]

$$\begin{aligned} S_x(z) &= -Q_x(z)d_{xa}(z) + \beta_0 d'_{xa}(0) \\ &= -Q_x(z)d_{xa}(0) + [\beta_0 - Q_x(z)z]d'_{xa}(0), \end{aligned} \tag{9}$$

where d'_{xa} represents the slope of the beam axis with respect to the z axis, and use has been made of the fact that in a uniform medium the rate of change of the amplitude displacement is constant while the displacement itself varies linearly with z. A similar equation would hold for $S_y(z)$ in a more general configuration.

3. SOLUTION OF THE BEAM EQUATIONS

Many solutions have been obtained for the parameters governed by Eqs. (5)–(7). The evolution of the beam parameter Q_x (or accordingly the spot size and phase front curvature) has been examined in greatest depth, while much less attention has been given to the detailed solutions of the displacement and phase parameter equations and their applications. It is now necessary to have solutions for all of these equations.

One can readily show that the solution to Eq. (5) has the familiar form

$$\frac{1}{q_x(z)} = \frac{1/q_{x1}}{1 + z/q_{x1}}, \tag{10}$$

where $1/q_{x1}$ is the initial ($z = 0$) value of $1/q_x(z)$. Similarly, one can show that the solutions of Eqs. (6) and (7) can be written as[39]

$$S_x(z) = \frac{S_{x1}}{1 + z/q_{x1}}, \tag{11}$$

$$P(z) = P_1 - \frac{i}{2}\ln\left(1 + \frac{z}{q_{x1}}\right) - \frac{S_{x1}^2 q_{x1}}{2\beta_0}\frac{z/q_{x1}}{1 + z/q_{x1}}, \tag{12}$$

where S_{x1} is the initial value of $S_x(z)$ and P_1 is the initial value of $P(z)$. When these parameter formulas are introduced into Eq. (4), one has a complete description of the propagation of the fundamental off-axis Gaussian beam in real uniform media.

The significance and applications of these results can be more readily explored by focusing on specific cases. It follows from Eq. (8) that if the starting position of the beam is at the beam waist ($R_{x1} = \infty$), the beam parameter there must be purely imaginary. By convention we use the notation $1/q_{x1} = -i/z_0$, where z_0 is the Rayleigh length. With this substitution Eq. (10) becomes

$$\frac{1}{q_x(z)} = \frac{-i/z_0}{1 - iz/z_0}. \tag{13}$$

When combined with Eq. (8), Eq. (13) yields the standard formulas for the propagation of the spot size and the phase front curvature, and Eqs. (11) and (12) become

$$S_x(z) = \frac{S_{x1}}{1 - iz/z_0}, \tag{14}$$

$$P(z) = P_1 - \frac{i}{2}\ln\left(1 - \frac{iz}{z_0}\right) - \frac{S_{x1}^2 z_0}{2\beta_0}\frac{z/z_0}{1 - iz/z_0}. \tag{15}$$

The parameter functions given in Eqs. (13)–(15) can now be combined with Eqs. (8) and (9) and substituted into Eq. (4). After some arithmetic one finds that the result can be written as[39]

$$
\begin{aligned}
&A(x', z') \\
&= A_0 \exp\left\{\left[-\frac{1}{w_0'^2(1+z'^2)} - i\frac{z'}{w_0'^2(1+z'^2)}\right]x'^2\right. \\
&\quad + \left[\frac{2(p_1 + z'v_1)}{w_0'^2(1+z'^2)}\right. \\
&\quad \left. + i\frac{2z'(p_1 + z'v_1)}{w_0'^2(1+z'^2)} - i\frac{2v_1}{w_0'^2}\right]x' \\
&\quad + \left[-\ln(1+z'^2)^{1/4} - \frac{z'^2(v_1^2 - p_1^2) + 2z'v_1p_1}{w_0'^2(1+z'^2)}\right. \\
&\quad \left.\left. + i\frac{z'(v_1^2 - p_1^2) - 2z'^2v_1p_1}{w_0'^2(1+z'^2)} + \frac{i}{2}\tan^{-1}(z')\right]\right\},
\end{aligned}
\tag{16}
$$

where we have used the formula for the Rayleigh length in terms of the spot size at the beam waist $z_0 = n\pi w_0^2/\lambda$ to eliminate the propagation constant $\beta_0 = 2\pi n/\lambda$, with n being the index of refraction of the medium within the waveguide. It has been convenient to normalize distances in the direction of propagation with respect to the Rayleigh length by introducing the normalized distance $z' = z/z_0$. It has also been helpful to normalize all transverse distances to the waveguide wall separation d, and thus we have introduced the normalized transverse coordinate $x' = x/d$, the normalized spot size $w_0' = w_0/d$, the initial position in the x direction $p_1 = d_{xa}/d$, and the rate of change of this position with respect to normalized distance in the z direction $v_1 = dp_1/dz'$. The initial value of the phase has arbitrarily been set equal to zero.

It is convenient for many purposes to deal with the intensity of the beam rather than the amplitude. We define the intensity by the relation

$$I(x', z') = A^*(x', z')A(x', z'), \tag{17}$$

where the asterisk means complex conjugate. We choose the amplitude coefficient A_0 of the off-axis Gaussian beam given in Eq. (16) so that $I(x', z')$ will be normalized according to the integral

$$\int_{-\infty}^{\infty} I(x', z')\mathrm{d}x' = 1. \tag{18}$$

After some further arithmetic one finds that the normalized field can be written as

$$
\begin{aligned}
A(x', y') = &\left[\frac{(2/\pi)^{1/2}}{w_0'(1+z'^2)^{1/2}}\right]^{1/2} \\
&\times \exp\left\{-\left[\frac{x' - (p_1 + z'v_1)}{w_0'(1+z'^2)^{1/2}}\right]^2\right\} \\
&\times \exp\left(-i\left\{z'\left[\frac{x' - (p_1 + z'v_1)}{w_0'(1+z'^2)^{1/2}}\right]^2\right.\right. \\
&\left.\left. + \frac{2v_1x' - z'v_1^2}{w_0'^2} - \frac{1}{2}\tan^{-1}(z')\right\}\right).
\end{aligned}
\tag{19}
$$

Equation (19) with its preceding definitions is a complete solution for an off-axis Gaussian beam propagating in a real spatially homogeneous medium.

4. PROPAGATION IN WAVEGUIDES

We now have an analytical description of a Gaussian beam that propagates displaced and at a small angle with respect to an arbitrary z axis. This analysis has not yet included the possibility of reflecting surfaces in the beam path, but it is possible to start from this solution and determine the fields in the vicinity of such surfaces. The basic idea is to use a superposition of solutions of the type given above. Because the wave equation as employed here is linear, any superposition of solutions is also a solution.

It will be assumed that each reflecting surface is a flat high reflector as might be achieved with a metal waveguide for grazing angles of incidence. The electromagnetic boundary condition for such a surface is that the tangential component of the electric field must go to zero at the boundary. Thus for fields polarized parallel to the surface the amplitude of the fields must go to zero at the boundary. We will refer to this as the parallel polarization (electric field vector normal to the plane of incidence). For the perpendicular polarization (electric field vector in the plane of incidence), the field may have a local maximum or minimum at the boundary. It follows from these considerations that a representation for a guided parallel-polarized field requires that we find some superposition of Gaussian beams such that the fields all cancel at the locations of the boundaries. Such a superposition would satisfy the paraxial wave equation and would also by design satisfy the boundary conditions of the problem.

To be specific, it is assumed that the reflecting surfaces are exactly parallel to the z axis, while the beam itself may be propagating at a small angle with respect to this axis, as shown in Fig. 1. Initially, we will also focus on parallel-polarized beams. For this case, one finds that an amplitude superposition satisfying the boundary conditions at a single boundary is

$$A_{\parallel}(x', z') = A(x', z') - A(1 - x', z'). \tag{20}$$

It is clear from this formula that at an x' value of 0.5 the two components of the superposition cancel. Physically, this formula represents two Gaussian beams that are images of each other and for which the respective z axes are separated by the distance d. This distance was also chosen above as the normalization distance for the transverse beam and coordinate variables.

For the waveguide problem of interest here, one must account for multiple reflections at both boundaries. For this case Eq. (20) must be generalized to the superposition

$$
\begin{aligned}
A_{\parallel}(x', z') = &A(x', z') - A(1 - x', z') + A(2 + x', z') \\
&- A(3 - x', z') + \cdots - A(-1 - x', z') \\
&+ A(-2 + x', z') - A(-3 - x', z') + \cdots \\
= &\sum_{n=-N}^{+N} (-1)^n A[n + (-1)^n x', z'].
\end{aligned}
\tag{21}
$$

This summation ensures that the total electric field goes to zero at the two waveguide surfaces ($x' = -0.5, 0.5$). The necessary size of the summation limit N depends on the maximum transverse extent that the beam would occupy in the absence of the waveguide walls.

It is more convenient to focus on the intensities associated with the fields rather than their amplitudes. For the parallel polarization the intensity from Eq. (17) is now defined by

$$I_{\|}(x', z') = A_{\|}^{*}(x', z')A_{\|}(x', z'), \tag{22}$$

and Eqs. (19), (21), and (22) are the basis for Figs. 2–4. Figure 2 is a plot of a series of transverse intensity profiles for a normalized Gaussian beam that is undergoing diffraction and reflection from the flat waveguide surfaces located at the positions $x' = \pm 0.5$. The beam in this case is polarized parallel to the surfaces and enters directly along the waveguide axis. The waist spot size is $w_0' = 0.2$, and the propagation distance between successive profiles is $z' = 0.1$ (ten plots per Rayleigh length). This display format shows in a compact way the changes in beam intensity and width that occur with propagation. The intensity spreads into two symmetrical peaks and then returns to its initial near-Gaussian profile after approximately eight Rayleigh lengths. As required by the boundary condition, the intensity always remains zero at the reflecting surfaces.

Figure 3 is a plot of the transverse intensity profiles of an off-center Gaussian beam whose input waist occurs at the position $x' = 0.25$ (three fourths of the way to one side of the waveguide). The beam is again polarized parallel to the surface, and the waist spot size is $w_0' = 0.2$, but in this case the propagation distance between successive profiles is $z' = 1.0$ (one plot per Rayleigh length). The beam evolution is more complex than for the on-axis beam in Fig. 2, and recurrence is after approximately every 64 Rayleigh lengths. The beam reforms on the opposite side of the waveguide after approximately 32 Rayleigh lengths, and the 32 plots in the figure are intended only to illustrate the variety of profiles occurring at the intermediate distances.

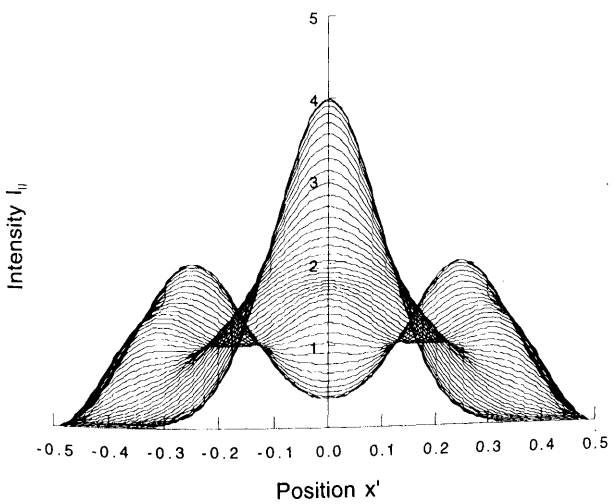

Fig. 2. Series of transverse intensity profiles of a normalized on-axis Gaussian beam interacting with flat waveguide surfaces located at the positions $x' = \pm 0.5$. The beam is polarized parallel to the surfaces, the waist spot size is $w_0' = 0.2$, and the propagation distance between successive profiles is $z' = 0.1$ (ten plots per Rayleigh length). The original near-Gaussian profile recurs after approximately eight Rayleigh lengths.

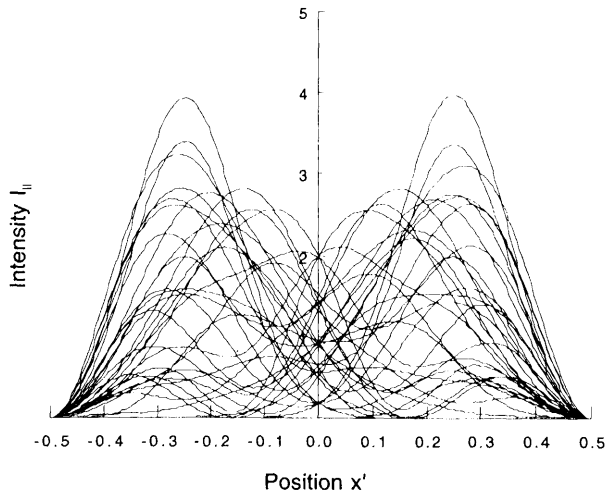

Fig. 3. Transverse intensity profiles of an off-center Gaussian beam whose input waist occurs at the position $x' = 0.25$. The beam is polarized parallel to the surface, the waist spot size is $w_0' = 0.2$, and the propagation distance between successive profiles is $z' = 1.0$. Recurrence is after approximately 64 Rayleigh lengths.

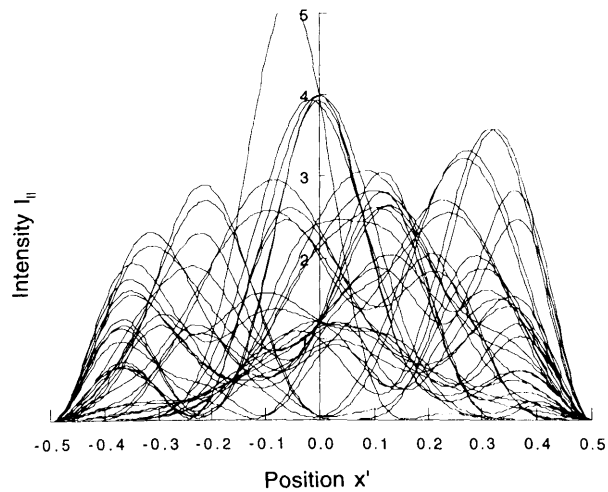

Fig. 4. Transverse intensity profiles of a misaligned Gaussian beam whose input waist occurs at the waveguide center $x' = 0$. The beam is polarized parallel to the surface, the waist spot size is $w_0' = 0.2$, the velocity of the input beam toward the right-hand surface is $v_1 = 0.1$, and the propagation distance between successive profiles is $z' = 1.0$. Recurrence is after approximately 64 Rayleigh lengths.

The effects of misalignment are shown in Fig. 4. In this case the input Gaussian beam is centered in the waveguide but is initially propagating toward the right-hand waveguide surface with a velocity $v_1 = 0.1$. As in Fig. 3, the waist spot size is $w_0' = 0.2$, the distance between plots is $z' = 1.0$, the number of plots given is 32, and recurrence is again at 64 Rayleigh lengths. It is perhaps notable that with partial sideways propagation at

the input, the intensity can achieve higher values than the peak input intensity, and in that respect a simple waveguide might have some use as a focusing element.

Similar results are obtained for the intensity of a beam that is polarized perpendicular to the reflecting surface. Instead of Eq. (20) the reflection at a single boundary in this case can be represented by the alternative superposition

$$A_\perp(x', z') = A(x', z') + A(1 - x', z'). \tag{23}$$

For the waveguide problem, one must again account for reflections at both boundaries. For this case Eq. (23) must be generalized to the superposition

$$\begin{aligned} A_\perp(x', z') &= A(x', z') + A(1 - x', z') + A(2 + x', z') \\ &\quad + A(3 - x', z') + \cdots + A(-1 - x', z') \\ &\quad + A(-2 + x', z') + A(-3 - x', z') + \cdots \\ &= \sum_{n=-N}^{+N} A[n + (-1)^n x', z']. \end{aligned} \tag{24}$$

This summation ensures that a maximum or minimum of the total electric field occurs at the waveguide surfaces ($x' = -0.5, 0.5$) or equivalently that the normal derivative of the field goes to zero.

For this perpendicular polarization the intensity is defined by

$$I_\perp(x', z') = A_\perp^*(x', z')A_\perp(x', z'), \tag{25}$$

and Eqs. (19), (24), and (25) are the basis for Figs. 5–7. In Fig. 5 is a plot of a series of intensity profiles for a perpendicular-polarized on-axis beam for which the waist spot size is $w_0' = 0.2$, and the propagation distance between successive profiles is $z' = 0.1$. The intensity evolves through a pattern having equal intensities at the center and the waveguide surfaces to a pattern in which the intensity is concentrated at the surfaces only. This evolution continues until, after a total distance of approximately 16 Rayleigh lengths from the input, the original intensity distribution recurs. As required by the boundary conditions, the intensity derivative is always zero at the waveguide surfaces.

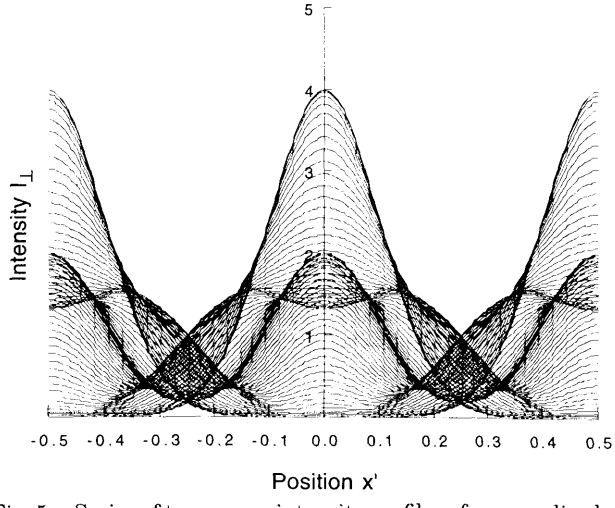

Fig. 5. Series of transverse intensity profiles of a normalized on-axis Gaussian beam. The beam is polarized perpendicular to the surfaces, the waist spot size is $w_0' = 0.2$, and the propagation distance between successive profiles is $z' = 0.1$. The original near-Gaussian profile recurs after approximately eight Rayleigh lengths.

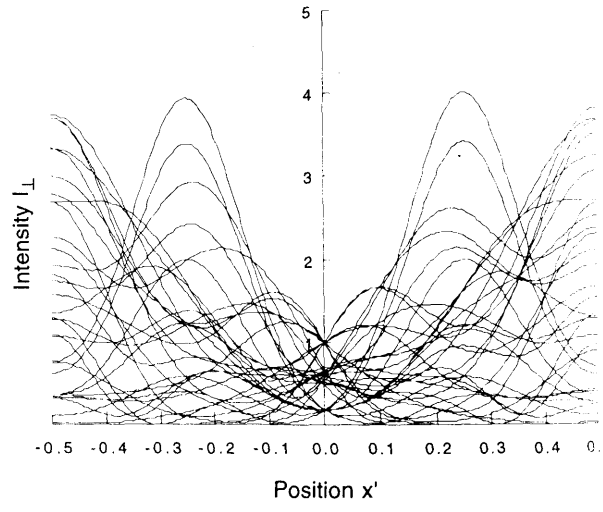

Fig. 6. Transverse intensity profiles of an off-center Gaussian beam whose input waist occurs at the position $x' = 0.25$. The beam is polarized perpendicular to the surface, the waist spot size is $w_0' = 0.2$, and the propagation distance between successive profiles is $z' = 1.0$. Recurrence is after approximately 64 Rayleigh lengths.

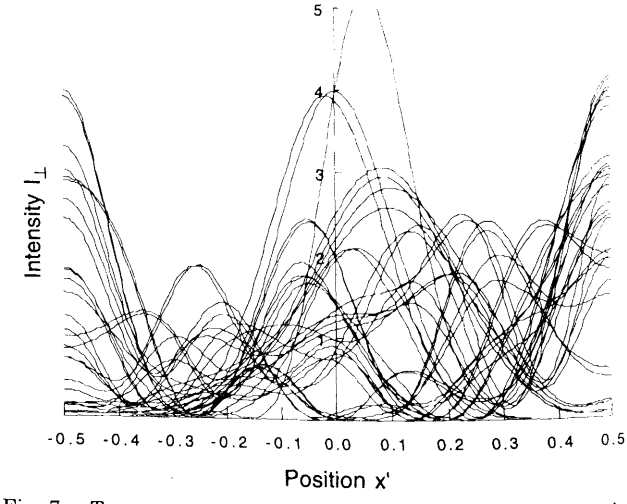

Fig. 7. Transverse intensity profiles of a misaligned Gaussian beam whose input waist occurs at the waveguide center $x' = 0$. The beam is polarized perpendicular to the surface, the waist spot size is $w_0' = 0.2$, the velocity of the input beam toward the right-hand surface is $v_1 = 0.1$, and the propagation distance between successive profiles is $z' = 1.0$. Recurrence is after approximately 64 Rayleigh lengths.

Figure 6 is a plot of the transverse intensity profiles of an off-center Gaussian beam whose input waist occurs at the position $x' = 0.25$. The beam is again polarized perpendicular to the surface, and the waist spot size is $w_0' = 0.2$, but in this case the propagation distance between successive profiles is $z' = 1.0$ (one plot per Rayleigh length). The beam evolution is more complex than for the on-axis beam in Fig. 5, and recurrence happens after approximately every 64 Rayleigh lengths. The beam re-

forms on the opposite side of the waveguide after approximately 32 Rayleigh lengths, and again the 32 plots in the figure are intended only to illustrate the variety of profiles occurring at the intermediate distances.

The effects of misalignment are shown in Fig. 7. In this case the input Gaussian beam is centered in the waveguide but is propagating toward the right-hand waveguide surface with a velocity $v_1 = 0.1$. The waist spot size is again $w_0' = 0.2$, the distance between plots is $z' = 1.0$, the number of plots given is 32 and recurrence is at 64 Rayleigh lengths. It may be seen that, as with parallel polarization, partial sideways propagation at the input can lead to intensities higher than the peak input intensity.

5. WAVEGUIDE MODES

The preceding discussions here have been concerned especially with the paraxial propagation of fields in waveguides when the input field is in the form of a Gaussian beam with spherical phase fronts. The waveguide propagation of these fields has been interpreted in terms of a superposition of fundamental Gaussian beams. An alternative analysis can be based on an expansion of the input beam in a set of waveguide eigenmodes. Although this expansion method would often be less efficient numerically than the Gaussian beam method, it provides a more direct perspective on the recurring nature of the fields.

As with the Gaussian beam solutions, it is sufficient to restrict attention to a two-dimensional, or parallel-plate, waveguide configuration. In the paraxial approximation the equations governing the x and y field variations of a rectangular waveguide are separable, so focusing on just the x variation does not represent a loss of generality. It is assumed at the outset that the field amplitude $A(x, z)$ can be written in the form

$$A(x, z) = B(x)\exp(-i\gamma z), \tag{26}$$

where, for the propagating modes, γ is a real quantity representing the modal correction to the plane-wave phase. If Eq. (26) is substituted into Eq. (3), the transverse part of the paraxial-wave equation is

$$\frac{d^2B}{dx^2} - 2\beta_0\gamma B = 0. \tag{27}$$

If the x coordinate is now imagined to have its origin at one of the waveguide surfaces, it is natural to express the solutions of Eq. (27) in the form

$$B(x) = a\sin k_x x + b\cos k_x x. \tag{28}$$

When Eq. (28) is substituted into Eq. (27), one obtains the characteristic equation

$$k_x^2 + 2\beta_0\gamma = 0. \tag{29}$$

As noted above, if the electric field is polarized parallel to the waveguide surfaces, the amplitude must go approximately to zero at those surfaces. For a waveguide spacing of d, the field solution is therefore of the form

$$B(x) = a\sin k_x x, \tag{30}$$

where the propagation constant k_x must satisfy the condition

$$k_x d = m\pi, \tag{31}$$

with $m = 1, 2, 3, \ldots$, and m is the mode index. Equations (29) and (31) may be combined to obtain the condition

$$-i\gamma z = \frac{i}{2\beta_0}\frac{m^2\pi^2}{d^2}z. \tag{32}$$

An arbitrary input field distribution can be expanded in terms of the waveguide modes. In the more general cases one may expect a nonzero amplitude for many of the lower-order waveguide modes in such an expansion. A condition of interest occurs when the phase delay implied by Eqs. (26) and (32) is an integer multiple of 2π:

$$\frac{1}{2\beta_0}\frac{m^2\pi^2}{d^2}z = 2h\pi, \tag{33}$$

where h is an integer. Also, the total field of a mode superposition (except for phase) will repeat if the phase differences between all of the component modes differ from each other by integer multiples of 2π.

The largest common divisor of the differences between adjacent terms in an m^2 series is unity. Thus the condition given in Eq. (33) will first occur simultaneously for all modes at the distance corresponding to $m = h = 1$:

$$z = \frac{4\beta_0 d^2}{\pi}. \tag{34}$$

If this distance is normalized to the Rayleigh length with the spot size normalized to the waveguide width, the result is

$$z' = \frac{8}{\pi w'^2}. \tag{35}$$

For $w' = 0.2$ as in Figs. 3 and 4, the distance from Eq. (35) is $z' = 63.66$. This is just the distance after which an off-axis Gaussian beam reappears as found in the numerical solutions leading to Figs. 3 and 4.

For some special input beams the repetition distance may be much shorter than the value given in Eq. (35). For example, with a symmetric on-axis beam, the mode index in Eq. (31) takes on only odd values. The largest common divisor of the differences between adjacent odd terms in an m^2 series is eight. Thus in place of Eq. (35) a parallel-polarized symmetric Gaussian beam recurs in the normalized distance $z' = (\pi w'^2)^{-1}$. For $w' = 0.2$ the recurrence distance is $z' = 7.96$, and this result is consistent with the numerical solutions given in Fig. 2.

If the electric field is polarized perpendicular to the waveguide surfaces, the derivative of the field will approximately vanish at the surfaces. For a waveguide spacing of d, the field solution from Eq. (28) in this case is of the form

$$B(x) = b\cos k_x x, \tag{36}$$

where the propagation constant k_x must satisfy the condition given in Eq. (31) with $m = 0, 1, 2, \ldots$, and m is again the mode index. In this case the normalized dis-

tance for the beam to recur is again given by Eq. (35), and the recurrence distance of $z' \cong 64$ for a spot size of $w' = 0.2$ is consistent with the numerical solutions leading to Figs. 6 and 7.

For special input beams the recurrence distance may again be much less than the value given in Eq. (35). With a symmetric on-axis beam, the mode index in Eq. (31) takes on only even values. The largest common divisor of the differences between adjacent even terms in an m^2 series is 4. Thus, in place of Eq. (35), a perpendicular-polarized symmetric Gaussian beam recurs in the normalized distance $z' = 2(\pi w'^2)^{-1}$. For $w' = 0.2$ the recurrence distance is $z' = 15.92$, and this result is consistent with the numerical solutions given in Fig. 5.

6. DISCUSSION

Gaussian beams have proven to be extremely useful for the propagation of localized electromagnetic signals. It is usually understood that such beams are not relevant to propagation in hollow metal waveguides. While continuing Gaussian beams cannot be solutions for such guides, recurring Gaussian beams can be. With proper design a free-space Gaussian beam can be efficiently coupled into a metal waveguide and, after a somewhat complex evolution, will emerge again into free space as a conventional Gaussian beam. A guiding configuration of this type can be useful when other low-loss guiding media are not available.

It is of interest to consider the actual dimensions that might be involved in constructing a waveguide to support recurring Gaussian beams at CO_2 laser wavelengths. It is clear from the input Gaussian beam shown in Fig. 2 that with a normalized waist spot size of $w_0' = 0.2$, truncation by the guide is extremely small, and for some purposes larger values of w_0' would be acceptable. Nevertheless, for consistency with our numerical results we will assume that the input beam has a normalized spot size of $w_0' = 0.2$. Then, if the input spot size were 1 mm, it follows that the waveguide width would be 5 mm. Under these very realizable conditions an on-axis beam in a planar waveguide would recur after either eight or sixteen Rayleigh lengths, depending on whether it were parallel or perpendicular polarized, respectively. (A rectangular guide with a possibly astigmatic input beam should be designed so that the parallel and perpendicular field recurrences are at the same plane.) The Rayleigh length in meters for this case would be $z_0 = \pi w_0^2/\lambda = \pi(10^{-3})^2/10.6 \times 10^{-6} = 0.3\,\mathrm{m}$, and eight Rayleigh lengths would correspond to a propagation distance of ~2.4 m. On the other hand, if the input spot size had the smaller value of 0.1 mm, the waveguide width would be 0.5 mm, and recurrence would be at 2.4 cm. These values appear to be in the range of typical CO_2 waveguide experiments.

The results obtained here are not limited in application to infrared optical signals, and applications would be possible wherever there was an absence of transparent waveguiding media. Thus, in the far-ultraviolet and the soft-x-ray regions, transparent materials are virtually unknown, whereas grazing reflectivities from metals can be quite high. Hollow metal waveguides have already been employed for the transmission of KrF excimer laser light.[42]

As a final comment, it may be noted that a similar phenomenon has been investigated in quantum mechanics. It follows from Schrödinger's equation that a localized wave function in free space will always tend to evolve and spread with time. However, if the wave function is initially localized within a potential well, the spreading cannot continue without limit. In fact, it has been shown that after a time interval the form of a wave function may experience a revival, and in ideal cases such revivals occur periodically.[43,44]

ACKNOWLEDGMENTS

This work was supported in part by the National Science Foundation under grant PHY94-15583. The author also expresses his appreciation to the members of The Institute of Optics and The Rochester Theory Center for Optical Science and Engineering at the University of Rochester for valuable discussions and hospitality during his sabbatical visit.

The author's permanent address is Department of Electrical and Computer Engineering and Department of Physics, Portland State University, P.O. Box 751, Portland, Oregon 97207-0751.

REFERENCES

1. G. D. Boyd and J. P. Gordon, "Confocal multimode resonator for millimeter through optical wavelength masers," Bell Syst. Tech. J. **40**, 489–508 (1961).
2. H. Kogelnik, "Imaging of optical modes—resonators with internal lenses," Bell Syst. Tech. J. **44**, 455–494 (1965).
3. H. Kogelnik, "On the propagation of Gaussian beams of light through lenslike media including those with a loss or gain variation," Appl. Opt. **4**, 1562–1569 (1965).
4. L. W. Casperson and S. D. Lunnam, "Gaussian modes in high loss laser resonators," Appl. Opt. **14**, 1193–1199 (1975), and references therein.
5. L. W. Casperson, "Beam modes in complex lenslike media and resonators," J. Opt. Soc. Am. **66**, 1373–1379 (1976).
6. A. A. Tovar and L. W. Casperson, "Generalized beam matrices: Gaussian beam propagation in misaligned complex optical systems," J. Opt. Soc. Am. A **12**, 1522–1533 (1995).
7. See for example, L. W. Casperson, D. G. Hall, and A. A. Tovar, "Sinusoidal-Gaussian beams in complex optical systems," J. Opt. Soc. Am. A **14**, 3341–3348 (1997).
8. V. G. Artyushenko, L. N. Butvina, V. V. Voitsekhovskii, E. M. Dianov, I. S. Lisitskii, A. M. Prokhorov, and V. K. Sysoev, "Polycrystalline waveguides with 0.35 dB/m losses at the 10.6 μm wavelength," Sov. J. Quantum Electron. **11**, 1–2 (1984).
9. K. Takahashi, N. Yoshida, and M. Yokota, "Optical fibers for transmitting high-power CO_2 laser beam," Sumitomo Electr. Tech. Rev. **23**, 203–210 (1984).
10. J. A. Harrington, J. C. Harrington, C. C. Gregory, and S. Harman, "Properties of alkali halide optical fibers," in *Optical Fibers in Medicine III*, A. Katzir, ed., Proc. SPIE **906**, 176–182 (1988).
11. B. B. Chaudhuri and D. K. Paul, "Wave propagation through a hollow rectangular anisotropic dielectric guide," IEEE J. Quantum Electron. **QE-14**, 557–560 (1978).

12. E. R. Dobrovinskaya, L. A. Litvinov, and Y. A. Rubinov, "Influence of thermal and mechanical effects on the properties of a sapphire hollow waveguide of IR waveguide lasers," Sov. J. Opt. Technol. **58**, 411–413 (1991).
13. M. Khelkhal and F. Herlemont, "Effective optical constants of alumina, silica and beryllia at CO_2 laser wavelengths," J. Opt. **23**, 225–228 (1992).
14. C. C. Gregory and J. A. Harrington, "High peak power CO_2 laser transmission by hollow sapphire waveguides," Appl. Opt. **32**, 3978–3980 (1993).
15. Y. Matsuura, T. Abel, and J. A. Harrington, "Optical properties of small-bore hollow glass waveguides," Appl. Opt. **34**, 6842–6847 (1995).
16. R. K. Nubling and J. A. Harrington, "Hollow-waveguide delivery systems for high-power, industrial CO_2 lasers," Appl. Opt. **35**, 372–380 (1996).
17. J. Dror, A. Inberg, R. Dahan, A. Elboim, and N. Croitoru, "Influence of heating on performances of flexible hollow waveguides for the mid-infrared," J. Phys. D **29**, 569–577 (1996).
18. C. D. Rabii and J. A. Harrington, "Optical properties of dual core hollow waveguides," Appl. Opt. **35**, 6249–6252 (1996).
19. E. Garmire, T. McMahon, and M. Bass, "Propagation of laser light in flexible hollow waveguides," Appl. Opt. **15**, 145–150 (1976).
20. E. Garmire, "Propagation of IR light in flexible hollow waveguides: further discussion," Appl. Opt. **15**, 3037–3039 (1976).
21. E. Garmire, T. McMahan, and M. Bass, "Low-loss optical transmission through bent hollow metal waveguides," Appl. Phys. Lett. **31**, 92–94 (1977).
22. E. Garmire, T. McMahon, and M. Bass, "Measurement of propagation in flexible infrared transmissive (FIT) waveguides," IEEE J. Quantum Electron. **QE-13**, 21–22 (1977).
23. T. Matsushima, I. Yamauchi, and T. Sueta, "Flexible infrared-transmissive plastic waveguides coated with evaporated aluminum," Jpn. J. Appl. Phys. **20**, 1345–1346 (1981).
24. J. Gombert and M. Gazard, "Attenuation characteristics of a planar dielectric coated metallic waveguide for 10.6 μm radiation," Opt. Commun. **58**, 307–310 (1986).
25. M. Miyagi and S. Karasawa, "A comparative study of rectangular and circular dielectric-coated metallic waveguides for CO_2 laser light: theory," Opt. Commun. **68**, 18–20 (1988).
26. S. V. Azizbekyan, V. G. Artyushenko, K. I. Kalaidzhyan, M. M. Mirakyan, and I. L. Pyl'nov, "Bending loss of hollow metal waveguides for mid-infrared range," Sov. Tech. Phys. Lett. **15**, 602–603 (1989).
27. S. Karasawa, M. Miyagi, T. Nakamura, H. Ishikawa, "Fabrication of dielectric-coated rectangular hollow waveguides for CO_2 laser light transmission," Trans. Inst. Electron. Inf. Commun. Eng. C-I **J72C-I**, 637–641 (1989).
28. S. V. Azizbekyan, V. G. Artyushenko, E. M. Dianov, K. I. Kalaidzhyan, and M. M. Mirakyan, "Transmission of hollow metal waveguides in the mid-infrared region," Sov. Phys. Tech. Phys. **35**, 392–393 (1990).
29. V. G. Artyushenko, K. I. Kalaidzhyan, M. M. Mirakyan, "Flexible hollow waveguides for the mid-IR range," Sov. Phys. Tech. Phys. **36**, 46–49 (1991).
30. H. Machida, H. Ishikawa, and M. Miyagi, "Low-loss lead fluoride-coated square waveguide for CO_2 laser light transmission," Electron. Lett. **27**, 2068–2070 (1991).
31. Y. Matsuura and M. Miyagi, "Bending losses and beam profiles of zinc selenide-coated silver waveguides for carbon dioxide laser light," Appl. Opt. **31**, 6441–6445 (1992).
32. H. Machida, Y. Matsuura, H. Ishikawa, and M. Miyagi, "Transmission properties of rectangular hollow waveguides for CO_2 laser light," Appl. Opt. **31**, 7617–7622 (1992).
33. Y. Matsuura and M. Miyagi, "Er:YAG, CO, and CO_2 laser delivery by ZnS-coated Ag hollow waveguides," Appl. Opt. **32**, 6598–6601 (1993).
34. T. Abel, J. Hirsch, and J. A. Harrington, "Hollow glass waveguides for broadband infrared transmission," Opt. Lett. **19**, 1034–1036 (1994).
35. Y. Matsuura, T. Abel, J. Hirsch, and J. A. Harrington, "Small-bore hollow waveguide for delivery of near single-mode IR laser radiation," Electron. Lett. **30**, 1688–1690 (1994).
36. R. K. Nubling and J. A. Harrington, "Hollow-waveguide delivery systems for high-power, industrial CO_2 lasers," Appl. Opt. **35**, 372–380 (1996).
37. D. Su, S. Somkuarnpanit, D. R. Hall, and J. D. C. Jones, "Thermal effects in a hollow waveguide beam launch for CO_2 laser power delivery," Appl. Opt. **35**, 4787–4789 (1996).
38. Jiwang Dal and J. A. Harrington, "High-peak-power, pulsed CO_2 laser light delivery by hollow glass waveguides," Appl. Opt. **36**, 5072–5077 (1997).
39. L. W. Casperson, "Grazing reflection of Gaussian beams," Appl. Opt. **38**, 554–562 (1999).
40. L. W. Casperson, "Gaussian light beams in inhomogeneous media," Appl. Opt. **12**, 2434–2441 (1973).
41. A. A. Tovar and L. W. Casperson, "Generalized beam matrices: Gaussian beam propagation in misaligned complex optical systems," J. Opt. Soc. Am. A **12**, 1522–1533 (1995), Eq. (24).
42. Y. Matsura and M. Miyagi, "Flexible hollow waveguides for delivery of excimer-laser light," Opt. Lett. **23**, 1226–1228 (1998).
43. J. H. Eberly, N. B. Narozhny, and J. J. Sanchez-Mondragon, "Periodic spontaneous collapse and revival in a simple quantum model," Phys. Rev. Lett. **44**, 1323–1326 (1980).
44. D. L. Aronstein and C. R. Stroud, Jr., "Fractional wavefunction revivals in the infinite square well," Phys. Rev. A **55**, 4526–4537 (1997), and references therein.